UNIVERSITAT POLITÈCNICA DE CATALUNYA
BARCELONATECH
Facultat d'Òptica i Optometria de Terrassa

GRAU EN ÒPTICA I OPTOMETRIA

TREBALL FINAL DE GRAU

MORPHOLOGICAL ANALYSIS FOR IMPROVING CLINICAL DIAGNOSIS OF SKIN CANCER

DANIEL ESPINAR MARTÍNEZ

MERITXELL VILASECA
FRANCISCO JAVIER BURGOS
DEPARTAMENT D'ÒPTICA I OPTOMETRIA

28 DE JUNY DE 2018

Facultat d'Òptica i Optometria de Terrassa

UNIVERSITAT POLITÈCNICA DE CATALUNYA
BARCELONATECH
Facultat d'Òptica i Optometria de Terrassa

GRAU EN OPTICA I OPTOMETRIA

La Dra. Meritxell Vilaseca y el Dr. Francisco Javier Burgos, com directors del treball,

CERTIFIQUEN

Que el Sr. Daniel Espinar Martínez ha realitzat sota la seva supervisió el treball "Morphological analysis for improving clinical diagnosis of skin cancer" que es recull en aquesta memòria per optar al títol de grau en Òptica i Optometria.

I per a què consti, signem aquest certificat.

Dra. Meritxell Vilaseca — Directora del TFG

Dr. Francisco Javier Burgos — Co-director del TFG

Terrassa, 6 de Juny de 2018

UNIVERSITAT POLITÈCNICA DE CATALUNYA
BARCELONATECH
Facultat d'Òptica i Optometria de Terrassa

GRAU EN OPTICA I OPTOMETRIA

MORPHOLOGICAL ANALYSIS FOR IMPROVING CLINICAL DIAGNOSIS OF SKIN CANCER

RESUM

Actualment, el diagnòstic del càncer de pell es realitza de forma visual; un especialista examina la lesió i els seus canvis mitjançant inspecció directa o fent servir un dermatoscopi. Si la lesió es considera sospitosa, s'ha d'extreure quirúrgicament per realitzar-ne la histologia i confirmar-ne el diagnòstic. Això comporta una elevada despesa hospitalaria, a part de ser un procés llarg i invasiu. En conseqüència, el principal objectiu d'aquest treball és estudiar si mitjançant tecnologia 3D i el posterior anàlisi morfològic de les lesions, es pot millorar el diagnòstic del càncer de pell. Amb aquesta finalitat, es van processar diferents lesions mesurades mitjançant un equip que incorporava tecnologia 3D en dos hospitals: l'Hospital Clínic i Provincial de Barcelona (Barcelona, Espanya) i la *Università degli Studi di Modena e Reggio Emilia* (Mòdena, Itàlia). En concret es van estudiar 608 lesions amb els següents diagnòstics: nevus, melanomes, carcinomes de cèl·lules basals, carcinomes de cèl·lules escamoses, queratosis seborreica i altres lesions benignes com angiomes, dermatofibromes i queratosis actínica. D'aquestes lesions es van obtenir diversos paràmetres com ara el volum, àrea, perímetre i altres valors de rugositat que, posteriorment, es van analitzar estadísticament.
D'acord als resultats obtinguts, hi ha diferències estadísticament significatives entre melanomes i nevus en termes de paràmetres d'àrea, volum i perímetre. Per tant, el sistema pot ajudar a millorar el diagnòstic del càncer de pell de forma no invasiva, especialment en el cas del melanoma que és el tipus més agressiu.

UNIVERSITAT POLITÈCNICA DE CATALUNYA
BARCELONATECH
Facultat d'Òptica i Optometria de Terrassa

GRAU EN OPTICA I OPTOMETRIA

MORPHOLOGICAL ANALYSIS FOR IMPROVING CLINICAL DIAGNOSIS OF SKIN CANCER

ABSTRACT

Nowadays, the diagnosis of skin cancer is made though visual inspection; a specialist examines the lesion and its changes by naked eye inspection or by using a dermatoscope. If the lesion is considered to be suspicious, it is excised surgically to perform its histology and confirm the diagnostic. This entails high hospital expenses, apart from being a long and invasive process. Consequently, the main objective of this work is to study whether through 3D technology and the subsequent morphological analysis of the lesions, the diagnosis of skin cancer can be improved. With this goal, different lesions were measured using a system that incorporated 3D technology at two hospitals: the Hospital Clínic i Provincial de Barcelona (Barcelona, Spain) and the *Università degli Studi di Modena e Reggio Emilia* (Modena, Italy). In particular, 608 lesions were studied including the following diagnostics: nevus, melanomas, basal cell carcinomas, squamous cell carcinomas, seborrheic keratosis, and other benign lesions such as angiomas, dermatofibromas and actinic keratosis. From these lesions, several parameters were obtained, such as the volume, area, perimeter and other roughness values, which were subsequently analyzed statistically. According to the results obtained, there are statistically significant differences between melanomas and nevi in terms of the parameters of area, volume and perimeter. Thus, the system can help to improve the diagnosis of skin cancer in a non-invasive way, especially in the case of melanoma that is the most aggressive type.

GRAU EN OPTICA I OPTOMETRIA

MORPHOLOGICAL ANALYSIS FOR IMPROVING CLINICAL DIAGNOSIS OF SKIN CANCER

RESUMEN

Actualmente, el diagnóstico del cáncer de piel se realiza de forma visual; un especialista examina la lesión y sus cambios mediante inspección directa o utilizando un dermatoscopio. Si la lesión se considera sospechosa, se debe extraer quirúrgicamente para realizar su histología y confirmar el diagnóstico. Esto conlleva un elevado gasto hospitalario, a parte de ser un proceso largo e invasivo. En consecuencia, el principal objetivo de este trabajo es estudiar si mediante tecnología 3D y el posterior análisis morfológico de las lesiones, se puede mejorar el diagnóstico del cáncer de piel. Para ello, se procesaron diferentes lesiones medidas mediante un equipo que incorporaba tecnología 3D en dos hospitales: el *Hospital Clínico y Provincial de Barcelona* (Barcelona, España) y la *Università degli Studi di Modena e Reggio Emilia* (Módena, Italia). En concreto se estudiaron 608 lesiones que incluían los siguientes diagnósticos: nevus, melanomas, carcinomas de células basales, carcinomas de células escamosas, queratosis seborreica y otras lesiones benignas como angiomas, dermatofibromas y queratosis actínica. De estas lesiones se obtuvieron varios parámetros tales como el volumen, área, perímetro y otros valores de rugosidad que, posteriormente, se analizaron estadísticamente. De acuerdo a los resultados obtenidos existen diferencias estadísticamente significativas entre melanomas y nevus en términos de los parámetros de área, volumen y perímetro. Por lo tanto, el sistema puede ayudar a mejorar el diagnóstico del cáncer de piel de forma no invasiva, especialmente en el caso del melanoma que es el tipo más agresivo.

UNIVERSITAT POLITÈCNICA DE CATALUNYA
BARCELONATECH
Facultat d'Òptica i Optometria de Terrassa

GRAU EN OPTICA I OPTOMETRIA

MORPHOLOGICAL ANALYSIS FOR IMPROVING CLINICAL DIAGNOSIS OF SKIN CANCER

RESUM EXTENS

INTRODUCTION

Skin cancer is an abnormal growth of skin cells and it is the most common human malignancy. Melanoma, which is one of the most aggressive skin cancer causing the greatest number of deaths, is one of the most rapidly increasing cancers in the world. In recent decades, more people have had skin cancer than all other cancers combined. Nevertheless, the 5 years survival rate for people with skin cancers can significantly improve if detected and treated early. For these reasons, the early diagnosis of skin cancer is very important.

Skin cancer is primarily diagnosed visually (a specialist examines the lesion changes to determine if these are likely to be a cancer or not) through direct inspection or using a dermoscope. The rule to inspect skin lesions through dermoscopy is the ABCDE, which outlines warning signs of the most common type of melanoma: A is for asymmetry, B is for border irregularity, C is for color, D is for the diameter and E for its evolution. However, the drawback of dermatoscopy is that it requires considerable training of the dermatologist in the interpretation of what it is seen. Unless the clinical exams draw firm conclusions, a skin biopsy is later required. A biopsy is effective, it determines if there are cancerous cells in a lesion and of which kind are they. A specialist in histology is needed as well, for treating the sample and identifying through his/her knowledge and experience what is wrong under the microscope. All these steps make it an expensive and long process. In this study, the outcomes of the 3D technology system included in a custom made multiphotonic platform with which a clinical study was conducted at two hospitals are analyzed and compared among skin cancer lesions of different etiology. The goal is to further investigate about the 3D morphological differences to clinically improve the detection of skin cancer.

METHODS AND MATERIALS

Multiphotonic platform and 3D system

A medical cart that integrates 4 photonic prototypes was developed at the CD6 for the diagnosis of skin cancer in the framework of the EU DIAGNOPTICS Project "Diagnosis of skin cancer using optics". One of them was a handheld 3D scanner prototype, based on a combination of two technologies: stereovision and structured light projection.

Processing of the lesions and computation of morphological parameters.

The Mountains Map Universal® software was used for processing the lesions, which included the removal of the tilt of a measure due to the fact that many of them were not strictly parallel to the skin surface, and the application of a zoom to remove the areas around the lesion and choose only the Region Of Interest (ROI). The unmeasured dots on the surface — since they had values out of the measurement range of the camera — were also filled with values of the neighboring pixels. Finally, the software also removed horizontal frequencies that corresponded to artifacts due to the patient's breathing, pulse or movement. The manual selection of the perimeter was performed later from the 2D image. Then, the area, volume, and perimeter were computed for each lesion using several algorithms available in the Mountains Map Universal® software. The program calculated the area and volume using three different algorithms; however, in order to facilitate the statistical analysis carried out in this study, an averaged area and volume were calculated from the three outcomes.

Afterwards, each 3D image was processed to obtain a series of specific representative profiles (~ 200) corresponding to the middle of the lesion approximately. The average of all these profiles was also computed.

Three profiles were finally taken at random and, for each of them, the following parameters related with the roughness of the lesion were calculated following the guidelines of the ISO 4287 standard.

- Pz: the maximum height of the profile within a sampling length (normal to the skin surface),
- Psk: the skewness asymmetry of the assessed profile,
- Pt: the total height of the profile on the evaluation length,
- Pa: the arithmetic mean deviation of the assessed profile,
- PSm: the mean width of profile elements, within a sampling length
- PPc: peak count, which are the number of peaks per centimeters, each peak being higher than the upper threshold, and falling under the lower threshold.

From the mean profile, the maximum height and the mean height for the highest positive value were also computed, as well as the maximum depth and the mean depth for the lowest negative value. The program gives the values of maximum height, the mean height and width for maximum, and the maximum depth, the mean depth and width for the minimum value.

In addition, two other customized parameters were calculated for each lesion as follows:

$$Ap = \frac{Areahole + Areapeak}{Perimetre} \quad Vp = \frac{Volumehole + Volumepeak}{Perimetre}$$

They were calculated as the sum of the areas/volumes of holes (concave curvature) and peaks (convex curvature), both calculated by one of the three methods formerly commented, and normalized by the lesion's perimeter. The purpose was to account for how much area/volume the lesion has with respect to its contour.

Samples acquisition

Clinical measurements of real skin lesions with the multiphotonic platform were acquired at the *Hospital Clínic i Provincial de Barcelona* (Barcelona, Spain) and the *Università degli Studi di Modena e Reggio Emilia* (Modena, Italy) from February 26, 2015 to December 15, 2016. All patients provided written informed consent before any examination and ethical committee approval was obtained. The study complied with the tenets of the 1975 Declaration of Helsinki (Tokyo revision, 2004). The lesions were diagnosed by dermatologists (SP and JM in Barcelona, GP and SB in Modena) using a commercial dermoscope and the confocal laser scanning microscope VivaScope® 1500 from MAVIG. When malignancy was suspected, the lesion was excised and a histological analysis was carried out.

Statistical analysis

The data were analyzed using the SPSS software for MAC (V.23.0. Armonk, NY: IBM Corp.). Comparisons were considered to be statistically significant for p values of less than 0.05. The Kolmogorov-Smirnoff test was used to evaluate the normal distribution of all variables. Since variables did not meet the criteria for normal distribution, the Kruskal-Wallis test was used to compare the data among groups of skin lesions, i. e., nevi, melanomas, BCCs etc. Furthermore, the Mann-Whitney U test was used to compare the main outcome measures between each group and any other.

RESULTS

608 skin lesions from patients of both hospitals were measured with the 3D scanner prototype. While 32% (194) of the lesions could be properly analyzed, the remaining 68% (414) could not, due to various reasons such as: many unmeasured points in the surface of the lesions; pronounced artifacts due to micro-movement while making the acquisition; lesions not properly centered that went out of the field of view, and hairs on the skin.

The diagnostics of the remaining 194 lesions that could be properly processed were the following: 81 (42%) corresponded to nevi (N) that were: melanocytic, dysplastic, blue, junctional or Spitz nevi; 60 (31%) were melanomas (MM); 18 (9%) basal cell carcinomas (BCC); 18 (9%) other benign lesions (BB), such as

angiomas, dermatofibromas and actinic keratosis; 11 (6%) seborrheic keratosis (SK); and 6 (3%) corresponded to squamous carcinomas (SCC).
The last three types of lesions (BB, SK, and SCC) were excluded from the analysis due to the low number of samples available in each category, which were not enough to perform a proper statistical analysis. For nevi (N), melanomas (MM) and BCCs, all analyzed parameters followed a non-normal distribution ($p<0.05$). Among all parameters computed, the Kruskal-Wallis test reported significant differences among lesions of different etiologies in terms of the area, volume, perimeter and parameters Ap and Vp ($p<0.001$). On the contrary, the parameters related with the roughness of the lesion that were calculated following the guidelines of the ISO 4287 did not provide significant differences ($p>0.05$) and, for this reason, they are no reported here.
Table 1 shows the mean of the parameters that reported significant differences, as well as the standard deviation (SD), and the range for each type of lesion individually and for N, MM and BCC altogether.

	MM	N	BCC	Total
Area	50,8 ± 38,4 (4,9-182,8)	28,6 ± 23,9 (2,9-127,3)	30,0 ± 18,0 (8,2-64,8)	37,2 ± 31,5 (2,9-182,8)
Volume	15,9 ± 39,6 (0,5-298,2)	5,8 ± 7,9 (0,2-37,6)	7,5 ± 7,4 (0,5-30,2)	9,797 ± 25,5 (0,2-298,2)
Perimeter	26,5 ± 10,9 (7,9-53,3)	18,9 ± 7,7 (6,6-44,4)	20,9 ± 6,5 (13,5-35,1)	21,9 ± 9,6 (6,6-53,3)
Ap	1,670 ± 0,638 (0,627-3,465)	1,404 ± 0,832 (0,457-7,095)	1,365 ± 0,529 (0,543-2,475)	1,500 ± 0,742 (0,457-7,095)
Vp	0,509 ± 1,874 (0,042-14,636)	0,198 ± 0,205 (0,022-1,424)	0,293 ± 0,280 (0,314-1,236)	0,326 ± 1,167 (0,022-14,636)

Table 1. Mean ± SD and (range: minimum, maximum) of the parameters that showed statistically significant differences among lesions.

We performed the Mann-Whitney U test, which allowed us to compare between pairs of types of lesions (Table 2). As it can be seen, when we compared MM vs. N all parameters showed statistically significant differences ($p<0.05$) meaning that melanomas and nevi are significantly different in terms of all these variables. On the other hand, regarding MM vs. BCC and N vs BCC, differences were not significant, meaning that it is difficult to distinguish a BCC from any other type of lesion (MM and N).

	P-VALUE				
Lesions / Parameters	**Area**	**Volume**	**Perimeter**	**Ap**	**Vp**
MM - N	< 0,001*	< 0,001*	< 0,001*	< 0,001*	< 0,001*
MM - BCC	0,034*	0,270	0,052	0,075	0,943
N - BCC	0,341	0,150	0,160	0,835	0,085
*Statisticaly significant					

Table 2. P-values of the Mann-Whitney U test.

The following figures (Figures 1, 2 and 3) show the boxplots for the area, volume and perimeter as well as *Ap* and *Vp* for the malignant lesions studied (MM and BCC) and the benign ones (N). MMs is the category that presents higher values of area, volume and perimeter.

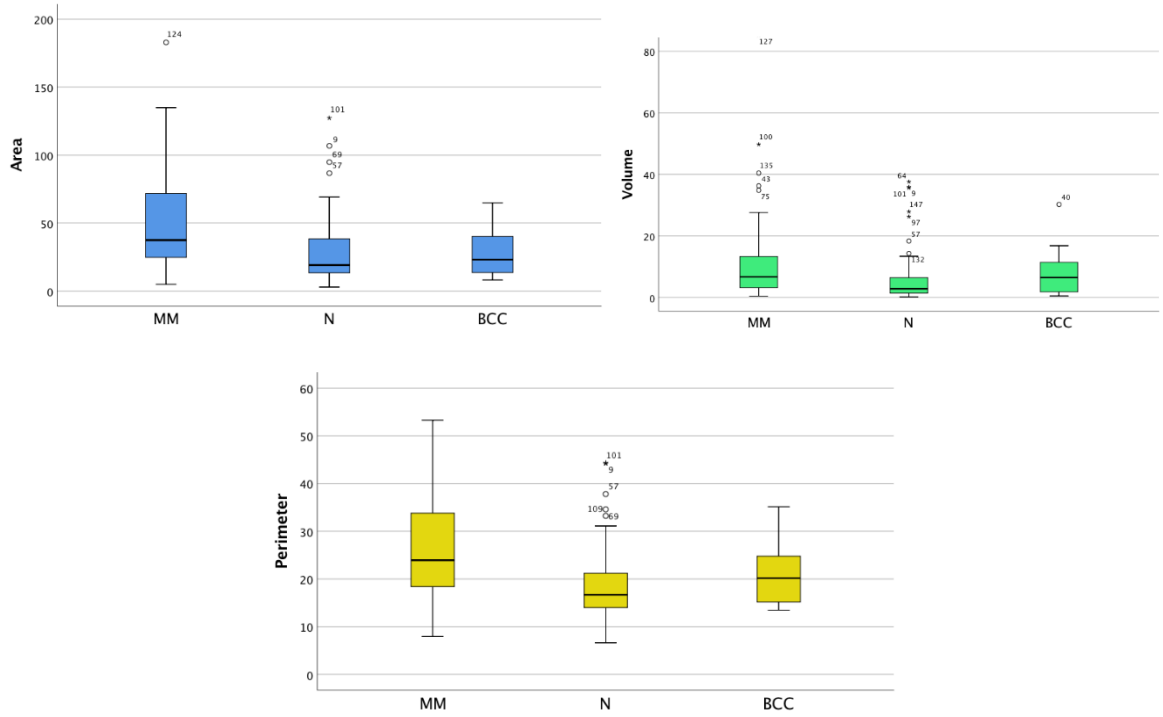

Figure 1. Boxplots of area (top left), volume (top right) and perimeter (bottom) of the different skin lesions. Five statistical descriptors are shown in these plots: maximum, third quartile, median, first quartile and minimum.

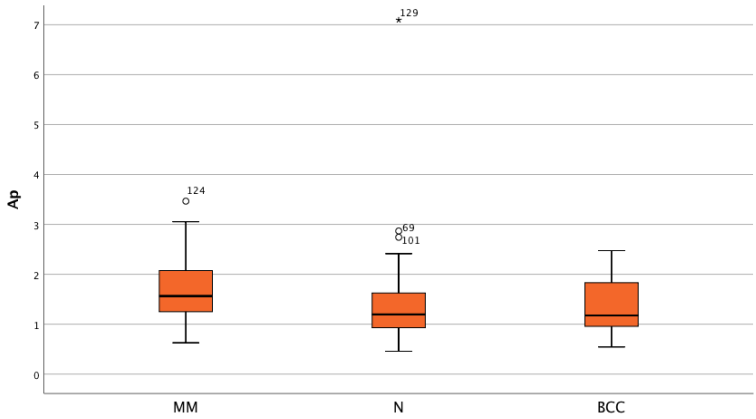

Figure 2. Boxplot of *Ap* of the different skin lesions. Five statistical descriptors are shown in these plots: maximum, third quartile, median, first quartile and minimum.

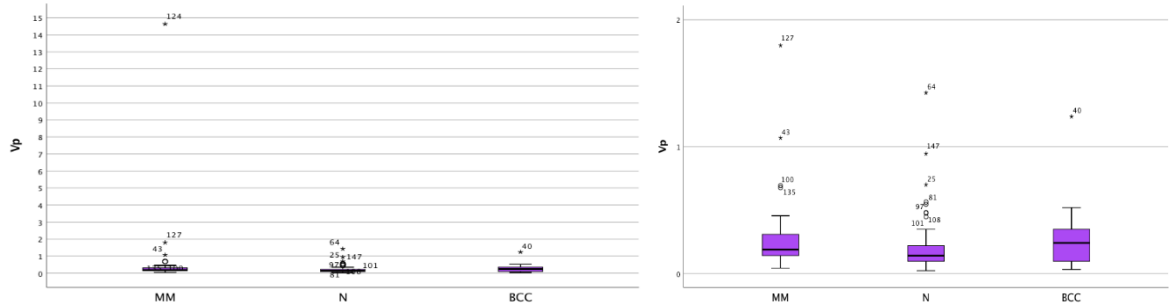

Figure 3. Boxplots of *Vp* of the different skin lesions (left) and the same but excluding outlier 124 in the case of the melanomas (right). Five statistical descriptors are shown in these plots: maximum, third quartile, median, first quartile and minimum.

It should also be noted that nevi is generally the type of lesion that presents more outliers (values out of the quartiles), which means a greater variability among samples.

The parameter *Ap* follow the same pattern as the previous ones (i. e., the area, volume and perimeter): malignant etiologies present the highest values although only significant differences can be established between MM and the other groups as commented above. Surprisingly, in the case of the *Vp* parameter, the median of the BCCs is higher than that of the MMs while the mean of the MMs is much higher than the one found for BCCs. A deeper analysis of this parameter reveals that there is one outlier in the MM group (124) with a value extremely high. Therefore, this parameter is not considered a reliable parameter.

It should be mentioned that the application of different algorithms of the Mountains Map Software was better (more robust) in computing the area than the volume. The repetition of measurements also revealed less dependency in the case of the area than in the volume. It is also important to highlight that that some of the steps of the process are done manually such as the Fourier filtering. With respect to the perimeter, it was seen that when the process was repeated, the result was practically the same. In this case, there is a manual selection of the ROI, too.

DISCUSSION

In this study, we analyzed the morphological parameters for improving clinical diagnosis of skin cancer using 3D technology, which is a non-invasive technique. Many skin lesions were analyzed but finally only 159 skin lesions were included in the statistical analysis. The 3D parameters of N, MM and BCC were analyzed by means of statistical tests. Results were especially good at differentiating MM from N, which is a very relevant aspect since they are the most difficult etiologies to differentiate from the clinical point of view due to their morphological similarities. Since the melanoma is the most dangerous type of skin cancer that can even lead to death, this result is very relevant. On the other hand, the results suggested that BCCs cannot be discriminated from MM and N using 3D technology. It is important to note that the area was found to be a

more reliable parameter than the volume, since it did not depend so much on how the processing was done.
According to this, our system can help to improve the diagnosis of skin cancer, especially melanoma. Through the area, the volume and the perimeter of the lesions, we can differentiate to a large extent whether a lesion is a melanoma or a nevus.
Future work will focus on taking into account other variables such as age or gender in the statistical analysis. And to analyze together 3D information with others also available in the medical cart, such as, spectral information, to improve even more the diagnosis capability of the system.

Morphological analysis for improving clinical diagnosis of skin cancer

DANIEL ESPINAR MARTÍNEZ[1]

[1]*Centre for Sensors, Instruments and Systems Development (CD6), Universitat Politècnica de Catalunya (Terrassa - Barcelona, Spain).*

**daniel.esma96@gmail.com*

Abstract: Nowadays, the diagnosis of skin cancer is made though visual inspection; a specialist examines the lesion and its changes by naked eye inspection or by using a dermatoscope. If the lesion is considered to be suspicious, it is excised surgically to perform its histology and confirm the diagnosis. This entails high hospital expenses, apart from being a long and invasive process. Consequently, the main objective of this work is to study whether through 3D technology and the subsequent morphological analysis of the lesions, the diagnosis of skin cancer can be improved. With this goal, different lesions were measured using a system that incorporated 3D technology at two hospitals: the Hospital Clínic i Provincial de Barcelona (Barcelona, Spain) and the *Università degli Studi di Modena e Reggio Emilia* (Modena, Italy). In particular, 608 lesions were studied including the following types: nevus, melanomas, basal cell carcinomas, squamous cell carcinomas, seborrheic keratosis, and other benign lesions such as angiomas, dermatofibromas and actinic keratosis. From these lesions, several parameters were obtained, such as the volume, area, perimeter and other roughness values, which were subsequently analyzed statistically. According to the results obtained, there are statistically significant differences between melanomas and nevi in terms of the parameters of area, volume and perimeter. Thus, the system can help to improve the diagnosis of skin cancer in a non-invasive way, especially in the case of melanoma that is the most aggressive type.

OCIS codes: (100.6890) Three-dimensional image processing; (170.1870) Dermatology; (120.3890) Medical optics instrumentation; (030.5770) Roughness

References and links

1. American Cancer Society. Cancer facts & figures 2016. Atlanta, American Cancer Society 2016.
2. Stern, R. (2010). Prevalence of a History of Skin Cancer in 2007. Arch Dermatol, 146(3).
3. BBC NEWS [Online]. Avaliable: http://news.bbc.co.uk/2/hi/health/5219540.stm
4. Guy GP, Machlin SR, Ekwueme DU, Yabroff KR. Prevalence and costs of skin cancer treatment in the U.S., 2002-2006 and 2007-2011. Am J Prev Med 2014; 104(4):e69-e74. doi:dx.doi.org/10.1016/j.amepre.2014.08.036.
5. P. Melia. (2017, Feb 20). The Skin Cancer Foundation [Online]. Available: http://www.skincancer.org.
6. A. Gadeliya Goodson and D. Grossman, "Strategies for early melanoma detection: Approaches to the patient with nevi," J. Am. Acad. Dermatol., vol. 60, no. 5, pp. 719–735, 2009.
7. G. Pellacani et al., "The impact of in vivo reflectance confocal microscopy for the diagnostic accuracy of melanoma and equivocal melanocytic lesions," J. Invest. Dermatol. 127(12), 2759–2765 (2007).
8. Delpueyo, X.; Vilaseca, M.; Royo, S.; Ares, M.; Rey-Barroso, L.; Sanabria, F.; Puig, S.; Malvehy, J.; Pellacani, J.; Noguero F.; et al. Multispectral imaging system based on light-emitting diodes for the detection of melanomas and basal cell carcinomas: A pilot study. J. Biomed. Opt. 2017, 22, 065006, doi:10.1117/1.JBO.22.6.065006.
9. M. Ares et al., "Handheld 3D scanning system for in-vivo imaging of skin cancer," in 5th Int. Conf. on 3D Body Scanning Technologies, pp. 231–236, Lugano, Switzerland(2014).
10. Berdic, N.; Dragan, D.; Mihic, S.; Anisic, Z. "Creation and usage of 3D full body avatars." International Journal of Engineering. Tome XV [2017] - Fascicule I [February] pp 29 - 34
11. X. Delpueyo, M. Vilaseca, S. Royo, M. Ares, F. Sanabria, J. Herrera, F. Burgos, J. Pujol, S. Puig, G. Pellacani, J. Vázquez, G. Solomita, and T. Bosch, "Handheld hyperspectral imaging system for the detection of skin cancer," in Midterm Meeting of the International Colour Association, Tokyo, Japan, 2015.
12. Xana, D.E. Development of a new spectral imaging system for the diagnosis of skin cancer. Doctoral Thesis, Technical University of Catalonia UPC-BarcelonaTech, Catalonia, 2017.
13. D. Malacara, Optical shop testing , 3rd edition, New Jersey: John Wiley & Sons Inc., 2007.
14. L. Tchvialeva, H. Zeng, I. Markhvida, D. I McLean, H. Lui, and T. Lee, "Skin Roughness Assessment", in Laboratory for Advanced Medical Photonics and Photomedicine Insitute, Department of Dermatology and Skin Science, University of British Columbia and Vancouver Coastal Health Research Institute, Vancouver, Canada.

1. Introduction

Skin cancer is an abnormal growth of skin cells and it is the most common human malignancy [1]. Melanoma, which is one of the most aggressive skin cancer causing the greatest number of deaths, is one of the most rapidly increasing cancers in the world. In recent decades, more people have had skin cancer than all other cancers combined [2]. The incidence of skin cancer is rapidly increasing in Europe, USA and Australia. The report of Global Burden of Disease of Solar Ultraviolet Radiation estimates that of the 60,000 deaths caused by skin cancer every year from excessive sunlight, 48,000 are caused by malignant melanomas and 12,000 by other skin cancers. [3] Nevertheless, the 5 years survival rate for people with skin cancers can significantly improve if detected and treated early. For these reasons, the early diagnosis of skin cancer is very important.

Due to the unreliability of dermoscopy and dermatologists caution, a lot of unnecessary surgical procedures are carried out, since a vast majority ends up in false positives. Also, it must be taken into account the high cost related with this procedure. The annual cost of treating skin cancers in the USA is estimated at $8.1 billion: about $4.8 billion for nonmelanoma skin cancers and $3.3 billion for melanoma. [4]
Each type of cancer has a different presentation, depending on the affected cell type and the stage at which the disease is recognized (fig 1):

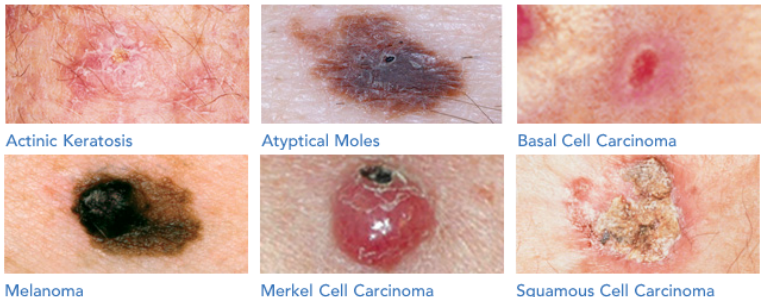

Figure 1. Different types of cancers and pre-cancers (Ref. [5]).

The following are the most common types of skin cancer:

Atypical Moles (Dysplastic Nevi) are non-cancerous moles that have some similarity with melanomas. The dysplastic nevus, is the easiest to cure if it is detected early. However, it may be difficult to distinguish between this kind of nevi and melanomas at the beginning stage.

Melanoma is the most dangerous form of skin cancer. In advanced stages, it is very dangerous; however, it is rare that melanoma becomes present without warning.

Basal Cell Carcinoma (BCC), which is the abnormal and uncontrolled growth of the basal cells, is the most common form of skin cancer and, in fact, is the most common type cancer of all kinds. The BCC takes the form of a sore, a red patch or a scar. However, the recovery in the first stages is completely successful.

Actinic keratosis (AK) or solar keratosis, is a common type of skin pre-cancer. It is called pre-cancer because it can be the first step towards a squamous cell carcinoma (SCC). The AK consists of an uncontrolled growth of squamous cells in the epidermis.

Seborrheic keratosis (SK) is a common skin growth. It may seem worrisome because it can look like a wart, pre-cancerous skin growth (actinic keratosis), or skin cancer. Despite their appearance, seborrheic keratoses are harmless.

Squamous Cell Carcinoma (SCC) is considered the second most common type of skin cancer, and consists of the abnormal and uncontrolled growth of squamous cells of the epidermis. The appearance of the SCCs are rough or scaly patches that are persistent and may bleed with a contusion. It can give us the feeling of warts or open sores with raised edges and a crusted surface.

Merkel Cell Carcinoma (MCC) is a very aggressive skin cancer, which has a higher mortality rate than melanoma but is less frequent. It has an elevated risk of recurrence and metastasis.

Skin cancer is primarily diagnosed visually (a specialist examines the lesion changes to determine if these are likely to be a cancer or not) through direct inspection or using a dermoscope, a handheld device with a magnifying lens and a white and uniform illumination field. The light is often polarized to remove specular reflection from the skin surface to capture information from deeper tissue layers. The rule to inspect skin lesions through dermoscopy is the ABCDE, which outlines warning signs of the most common type of melanoma: A is for asymmetry, B is for border irregularity, C is for color, D is for the diameter and E for its evolution. [6]

However, the drawback of dermatoscopy is that it requires considerable training of the dermatologist in the interpretation of what it is seen. Unless the clinical exams draw firm conclusions, a skin biopsy is later required. A biopsy is effective, it determines if there are cancerous cells in a lesion and of which kind are they. A specialist in histology is needed as well, for treating the sample and identifying through his/her knowledge and experience what is wrong under the microscope. All these steps make it an expensive and long process.

Accordingly, many efforts have been made in the last years to improve cancer diagnosis through the use of new optical technologies available, such as confocal microscopy [7], multispectral imaging [8] and 3D technology [9].

A recent study of the University of Queensalnd involved the use of 3D technology for skin lesion analysis: “The VECTRA Whole Body 360”, which allows a detailed 3-D skin image of a patient to be obtained. [10] The patient stands within a scaffold surrounded by 46 cameras that take an image simultaneously. A computer program then stitches the images together to produce the 3-D model that replicates the skin surface in complete detail. The main function is tracking changes in skin lesions, which can lead to a better diagnosis of skin cancer.

Another European project entitled DIAGNOPTICS "Diagnosis of skin cancer using optics" (seventh ICT PSP call for proposals 2013, 2014-2016) [11] carried out at the Centre for Sensors, Instruments and Systems Development (CD6) of the UPC had as the main objective the development of a multiphotonic diagnostic platform including multispectral and 3D techniques, optical feedback interferometry (OFI) and confocal microscopy to improve diagnosis and prognosis of skin cancer.

In this study, the outcomes of the 3D technology system included in the former platform are analyzed and compared among skin cancer lesions of different etiology. The goal is to further investigate about the 3D morphological differences to clinically improve the detection of skin cancer.

2. Methods and materials

2.1. Multiphotonic platform and 3D system

A medical cart that integrates four photonic prototypes was developed at the CD6 for the diagnosis of skin cancer in the framework of the DIAGNOPTICS project (Figure 2 left). One of them was a handheld 3D scanner prototype, based on a combination of two technologies: stereovision and structured light projection. It included two monochrome and one color cameras as well as a light picoprojetor, obtaining a field of view of 19 x 14 mm^2 [9]. The scanner also included a housing with the functions of protecting the optics and minimizing the effects of light reflections inside. The system also incorporated a computer with a software developed to acquire and process the 3D raw data.

The light picoprojector sequentially projects a set of sinusoidal patterns shifted over the skin and the recorded monochrome images are then processed by a conventional phase-shifting algorithm to obtain the wrapped phase maps [13]. Afterwards, from these phase maps, the 3D data is obtained by triangulation. Additionally to the geometric coordinates of the object points (X, Y, Z), the color information of the skin (R, G, B) is superimposed [12] in order to determine where the contour of the lesion is (2D image).

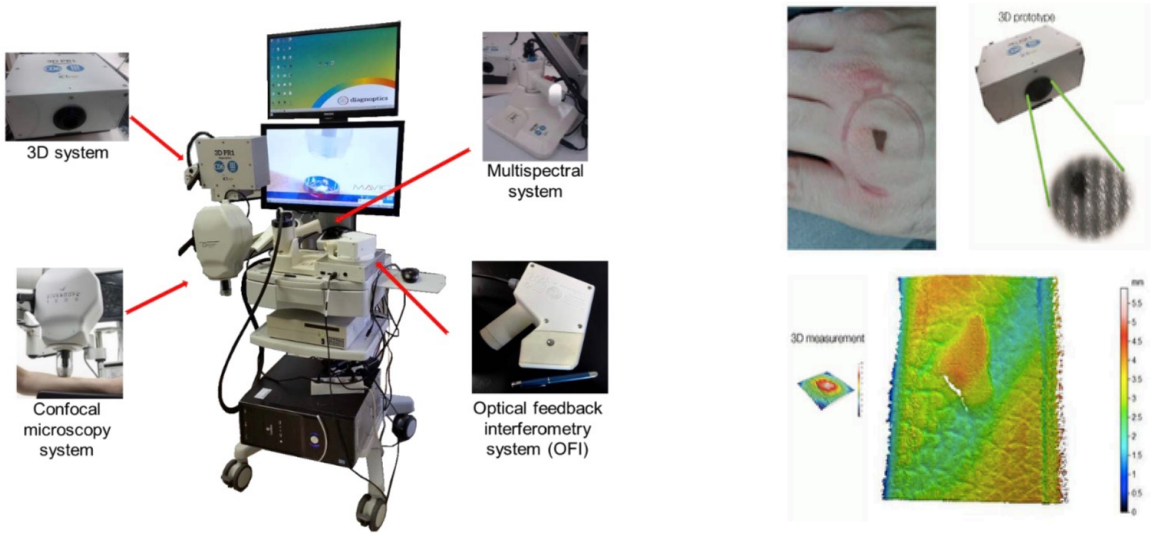

Figure 2: Medical cart (left) (Ref. [12]), and lesion and 3D prototype (top right) and topographic images of the skin and the lesion (bottom right) obtained with the 3D system.

2.2. Processing of the lesions and computation of morphological parameters.

The Mountains Map Universal® software was used for processing the lesions, which included the removal of the tilt of a measure due to the fact that many of them were not strictly parallel to the skin surface, and the application of a zoom to remove the areas around the lesion and choose only the Region Of Interest (ROI). The unmeasured dots on the surface — since they had values out of the measurement range of the camera — were also filled with values of the neighboring pixels. Finally, the software also removed horizontal frequencies that corresponded to artifacts due to the patient's breathing, pulse or movement (Figure 3).

The final 3D map of one lesion is shown in Figure 4 as an example as well as the manual selection of the perimeter that was performed later from the 2D color image. Then, the area, volume, and perimeter were computed for each lesion using several algorithms available in the Mountains Map Universal® software. The program calculated the area and volume using three different algorithms; however, in order to facilitate the statistical analysis carried out in this study, an averaged area and volume were calculated from the three outcomes.

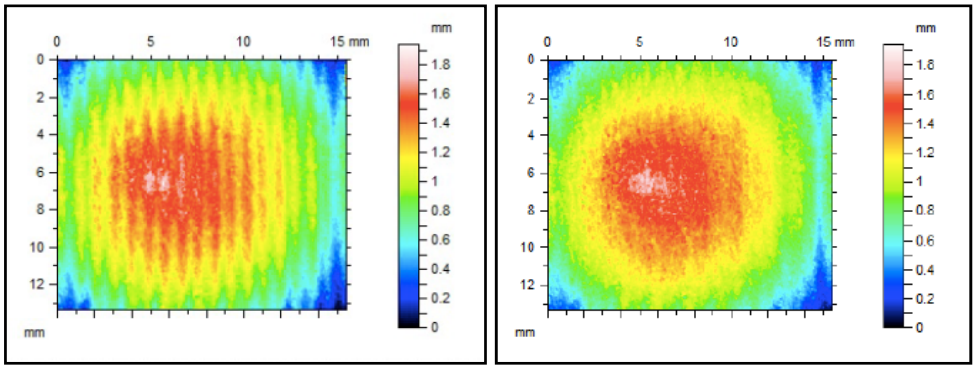

Figure 3: 3D image of a lesion before (left) and after the removal the unwanted horizontal frequencies that correspond to artifacts (right).

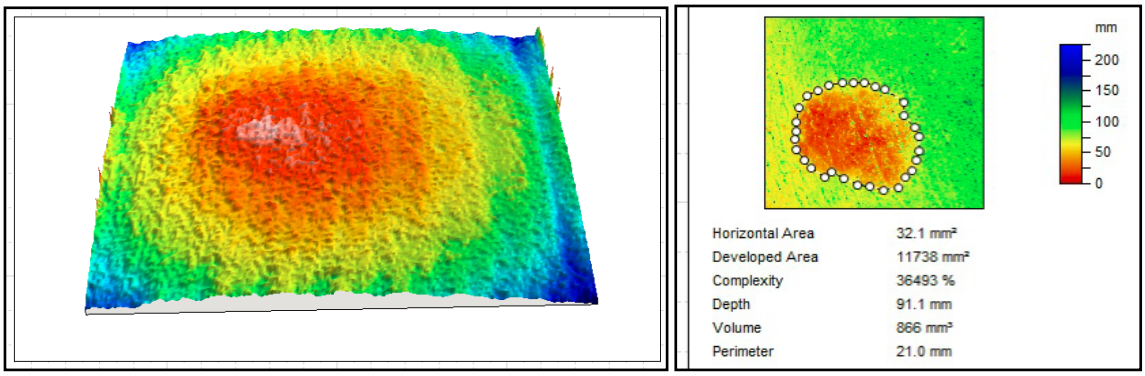

Figure 4: 3D map of a lesion finally obtained after processing (left) and manual outline from the 2D image (right).

Afterwards, each 3D image was processed to obtain a series of specific representative profiles (~ 200) corresponding to the middle of the lesion approximately (Figure 5). The average of all these profiles was also computed.

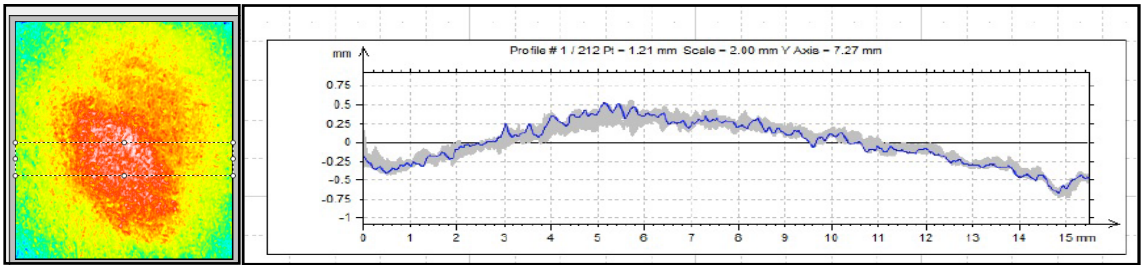

Figure 5: Region of the lesion from which the representative profiles are selected (left) and corresponding profiles (right). The mean profile is shown in blue.

Three profiles were finally taken from the set shown in Figure 5 at random and, for each of them, the following parameters, related with the roughness of the lesion, were calculated following the guidelines of the ISO 4287 standard [14]:

- Pz: the maximum height of the profile within a sampling length (normal to the skin surface),
- Psk: the skewness asymmetry of the assessed profile,
- Pt: the total height of the profile on the evaluation length,
- Pa: the arithmetic mean deviation of the assessed profile,
- PSm: the mean width of profile elements, within a sampling length
- PPc: peak count, which are the number of peaks per centimeters, each peak being higher than the upper threshold, and falling under the lower threshold.

From the mean profile, the maximum height and the mean height for the highest positive value were also computed, as well as the maximum depth and the mean depth for the lowest negative value (figure 6). In this figure, we can also see the average profile value with three underlined areas. The central zone corresponds to the maximum value of the average profile, while the two lateral zones correspond to the minimum values. The program gives the values of maximum height, the mean height and width for maximum, and the maximum depth, the mean depth and width for the minimum value. In this case, these three values correspond to the central zone, which is the maximum of the average profile value.

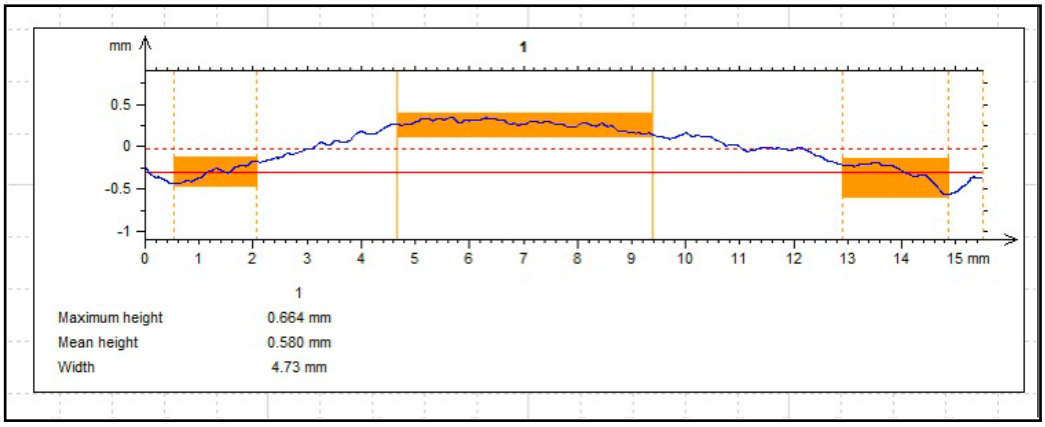

Figure 6: Average profile value with the values of: maximum height, mean height and width of the lesion.

In addition, two other customized parameters were calculated for each lesion as follows:

$$Ap = \frac{Areahole + Areapeak}{Perimetre} \qquad \text{Eq. (1)}$$

$$Vp = \frac{Volumehole + Volumepeak}{Perimetre} \qquad \text{Eq. (2)}$$

They were calculated as the sum of the areas/volumes of holes (concave curvature) and peaks (convex curvature), both calculated by one of the three methods formerly commented, and normalized by the lesion's perimeter. The purpose was to account for how much area/volume the lesion has with respect to its contour.

2.3. Samples acquisition

Clinical measurements of real skin lesions with the multiphotonic platform were acquired at the *Hospital Clínic i Provincial de Barcelona* (Barcelona, Spain) and the *Università degli Studi di Modena e Reggio Emilia* (Modena, Italy) from February 26, 2015 to December 15, 2016. All patients provided written informed consent before any examination and ethical committee approval was obtained. The study complied with the tenets of the 1975 Declaration of Helsinki (Tokyo revision, 2004). The lesions were diagnosed by dermatologists (SP and JM in Barcelona, GP and SB in Modena) using a commercial dermoscope and the confocal laser scanning microscope VivaScope® 1500 from MAVIG. When malignancy was suspected, the lesion was excised and a histological analysis was carried out. 608 skin lesions from patients of both hospitals were finally measured with the 3D scanner prototype of the medical card including nevi, melanomas, basal cell carcinomas (BCC), squamous carcinomas (SCC), seborrheic keratosis (SK), and other benign lesions (BB), such as angiomas, dermatofibromas and actinic keratosis.

2.4. Statistical analysis

The data were analyzed using the SPSS software for MAC (V.23.0. Armonk, NY: IBM Corp.). Comparisons were considered to be statistically significant for p values of less than 0.05. The Kolmogorov-Smirnoff test was used to evaluate the normal distribution of all variables. Since variables did not meet the criteria for normal distribution, the Kruskal-Wallis test was used to compare the data among groups of skin lesions, i. e., nevi, melanomas, BCCs etc. Furthermore, the Mann-Whitney U test was used to compare the main outcome measures between each group and any other.

3. Results

From the 608 skin lesions measured, 32% (194) could be properly analyzed while the remaining 68% (414) could not, due to various reasons such as: many unmeasured points in the surface of the lesions; pronounced artifacts due to micro-movement while making the acquisition; lesions not properly centered that went out of the field of view, and hairs on the skin.

The diagnostics of the remaining 194 lesions that could be properly processed were the following: 81 (42%) corresponded to nevi (N) that were: melanocytic, dysplastic, blue, junctional or Spitz nevi; 60 (31%) were melanomas (MM); 18 (9%) basal cell carcinomas (BCC); 18 (9%) other benign lesions (BB), such as angiomas, dermatofibromas and actinic keratosis; 11 (6%) seborrheic keratosis (SK); and 6 (3%) corresponded to squamous carcinomas (SCC).

The last three types of lesions (BB, SK, and SCC) were excluded from the analysis due to the low number of samples available in each category, which were not enough to perform a proper statistical analysis. It is important to note that the parameter that represents the mean width within a sampling length (PSm) could not be calculated for 28 lesions.

Therefore, for nevi (N), melanomas (MM) and BCCs, all analyzed parameters followed a non-normal distribution ($p<0.05$). Among all parameters computed, the Kruskal-Wallis test reported significant differences among lesions of different etiologies in terms of the area, volume, perimeter and parameters Ap and Vp ($p<0.001$). On the contrary, the parameters related with the roughness of the lesion that were calculated following the guidelines of the ISO 4287 did not provide significant differences ($p>0.05$) and, for this reason, they are no reported here.

Table 1 shows the mean of the parameters that reported significant differences, as well as the standard deviation (SD), and the range (minimum, maximum) for each type of lesion individually and for N, MM and BCC altogether.

	MM	N	BCC	Total
Area	50,8 ± 38,4 (4,9-182,8)	28,6 ± 23,9 (2,9-127,3)	30,0 ± 18,0 (8,2-64,8)	37,2 ± 31,5 (2,9-182,8)
Volume	15,9 ± 39,6 (0,5-298,2)	5,8 ± 7,9 (0,2-37,6)	7,5 ± 7,4 (0,5-30,2)	9,797 ± 25,5 (0,2-298,2)
Perimeter	26,5 ± 10,9 (7,9-53,3)	18,9 ± 7,7 (6,6-44,4)	20,9 ± 6,5 (13,5-35,1)	21,9 ± 9,6 (6,6-53,3)
Ap	1,670 ± 0,638 (0,627-3,465)	1,404 ± 0,832 (0,457-7,095)	1,365 ± 0,529 (0,543-2,475)	1,500 ± 0,742 (0,457-7,095)
Vp	0,509 ± 1,874 (0,042-14,636)	0,198 ± 0,205 (0,022-1,424)	0,293 ± 0,280 (0,314-1,236)	0,326 ± 1,167 (0,022-14,636)

Table 1. Mean ± SD and (range: minimum, maximum) of the parameters that showed statistically significant differences among lesions.

We performed the Mann-Whitney U test, which allowed us to compare between pairs of types of lesions (Table 2). As it can be seen, when we compared MM vs. N all parameters showed statistically significant differences ($p<0.05$) meaning that melanomas and nevi are significantly different in terms of all these variables. On the other hand, regarding MM vs. BCC and N vs BCC, differences were not significant, meaning that it is difficult to distinguish a BCC from any other type of lesion (MM and N).

	P-VALUE				
Lesions / Parameters	**Area**	**Volume**	**Perimeter**	**Ap**	**Vp**
MM - N	< 0,001*	< 0,001*	< 0,001*	< 0,001*	< 0,001*
MM - BCC	0,034*	0,270	0,052	0,075	0,943
N - BCC	0,341	0,150	0,160	0,835	0,085
*Statisticaly significant					

Table 2. P-values of the Mann-Whitney U test.

The following figures (Figures 7,8 and 9) show the boxplots for the area, volume and perimeter as well as *Ap* and *Vp* for the malignant lesions studied (MM and BCC) and the benign ones (N). MMs is the category that presents higher values of area, volume and perimeter.

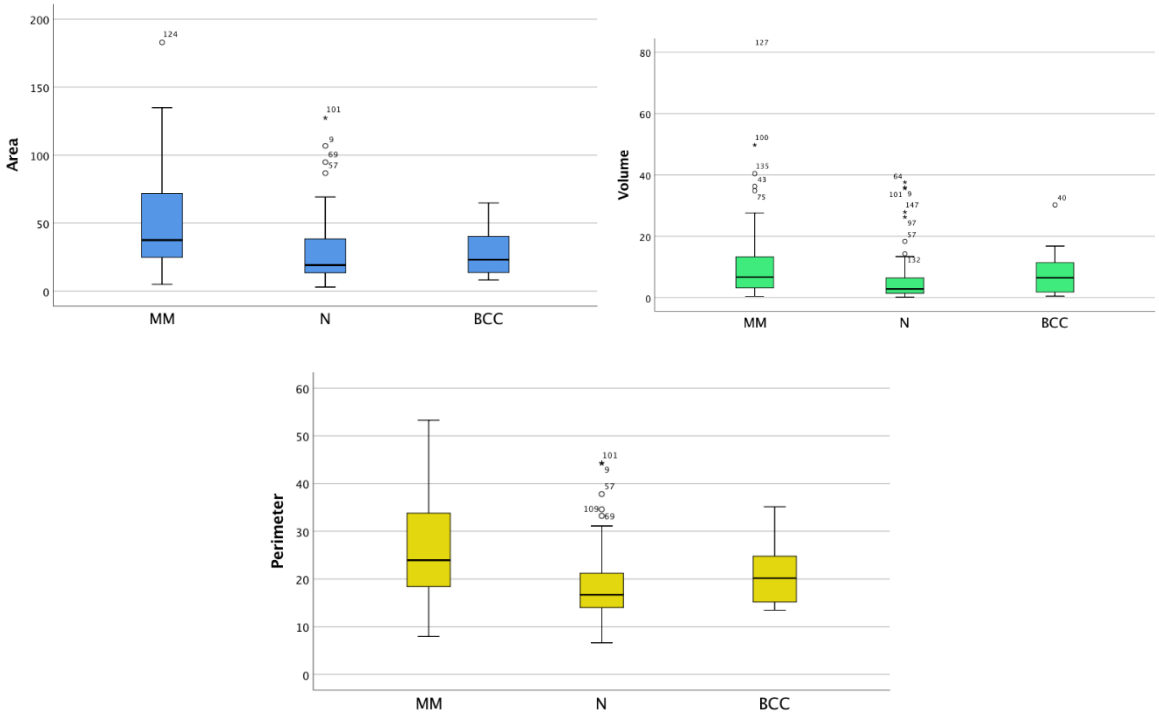

Figure 7. Boxplots of area (top left), volume (top right) and perimeter (bottom) of the different skin lesions. Five statistical descriptors are shown in these plots: maximum, third quartile, median, first quartile and minimum.

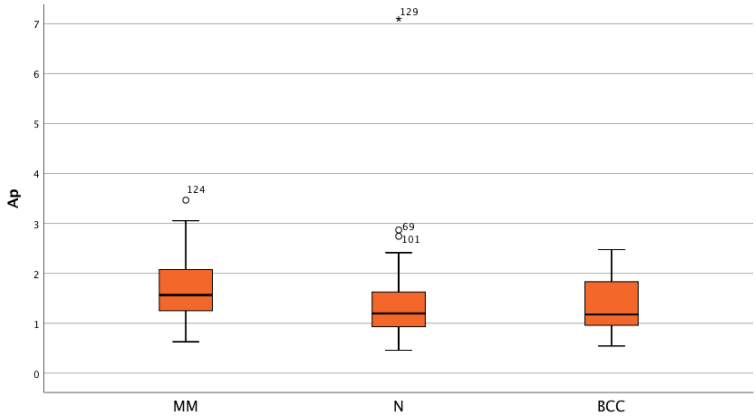

Figure 8. Boxplot of *Ap* of the different skin lesions. Five statistical descriptors are shown in these plots: maximum, third quartile, median, first quartile and minimum.

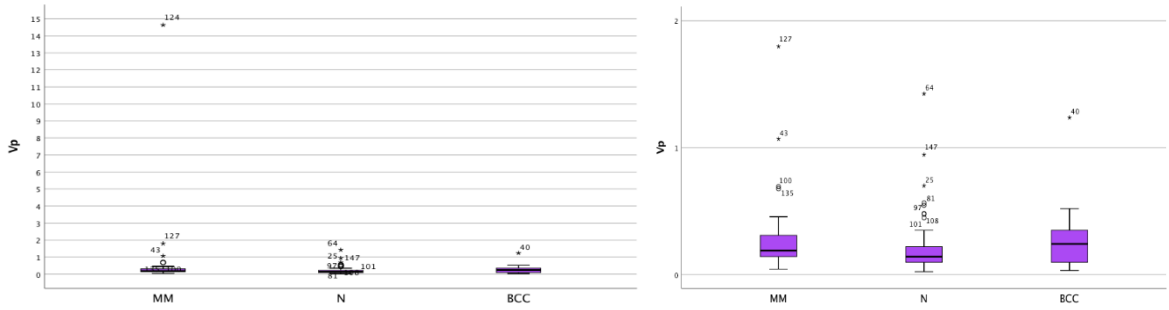

Figure 9. Boxplots of *Vp* of the different skin lesions (left) and the same but excluding outlier 124 in the case of the melanomas (right). Five statistical descriptors are shown in these plots: maximum, third quartile, median, first quartile and minimum.

It should also be noted that nevi is generally the type of lesion that presents more outliers (values out of the quartiles), which means a greater variability among samples. The parameter *Ap* follow the same pattern as the previous ones (i. e., the area, volume and perimeter): malignant etiologies present the highest values although only significant differences can be established between MM and the other groups as commented above.

Surprisingly, in the case of the *Vp* parameter, the median of the BCCs is higher than that of the MMs while the mean of the MMs is much higher than the one found for BCCs. A deeper analysis of this parameter reveals that there is one outlier in the MM group (124) with a value extremely high. Therefore, this parameter is not considered a reliable one.

It should be mentioned that the application of different algorithms of the Mountains Map Software was better (more robust) in computing the area than the volume. The repetition of measurements also revealed less dependency in the case of the area than in the volume. Moreover, it is also important to highlight that some of the steps of the process were done manually such as the Fourier filtering. With respect to the perimeter, it was seen that when the process was repeated, the result was practically the same. In this case, there is a manual selection of the ROI, too.

4. Discussion

In this study, we analyzed the morphological parameters for improving clinical diagnosis of skin cancer using 3D technology, which is a non-invasive technique.

Many skin lesions were analyzed but finally only 159 skin lesions were included in the statistical analysis: 81 nevi (N), 60 melanomas (MM), and 18 basal cell carcinomas (BCC). 414 could not be processed due to various reasons such as: many unmeasured points in the surface of the lesions; pronounced artifacts due to micro-movement while making the acquisition; lesions not properly centered that went out of the field of view, and hairs on the skin. Other 18 benign lesions (BB), 11 seborrheic keratosis (SK), and 6 squamous carcinomas (SCC) were also excluded due to the low number of samples available in each category.

The 3D parameters of these etiologies (N, MM and BCC) were analyzed by means of statistical tests. Results were especially good at differentiating MM from N, which is a very relevant aspect since they are the most difficult etiologies to differentiate from the clinical point of view due to their morphological similarities. Since the melanoma is the most dangerous type of skin cancer that can even lead to death, this result is very relevant. On the other hand, the results suggested that BCCs cannot be discriminated from MM and N using 3D technology. It is important to note that the area was found to be a more reliable parameter than the volume, since it did not depend so much on how the processing was done.

Nevertheless, BCCs can be differentiated more easily from a clinical point of view and, furthermore, they are not very aggressive so that dermatologists are more concerned in detecting MM at early stages than BCCs. According to this, our system can help to improve the diagnosis of skin cancer, especially melanoma. Through the area, the volume and the perimeter of the lesions, we can differentiate to a large extent whether a lesion is a melanoma or a nevus.

Future work will focus on taking into account other variables such as age or gender in the statistical analysis. And to analyze together 3D information with others also available in the medical cart, such as, spectral information [12], to improve even more the diagnosis capability of the system.

5. Acknowledgments

This research was supported by the Spanish Ministry of Economy and Competitiveness under the grants DPI2014-56850-R and DPI2017-89414-R, and by the European Union through the project DIAGNOPTICS 'diagnosis of skin cancer using optics' (ICT PSP seventh call for proposals 2013, 621066). Daniel Espinar would like to thank the AGAUR of the Generalitat de Catalunya for the collaboration research grant for university students he was awarded (call 2017-18).

Instructions for the preparation of a manuscript for OSA express journals

AUTHOR ONE,[1] AUTHOR TWO,[2,*] AND AUTHOR THREE[2,3]

[1]Peer Review, Publications Department, The Optical Society, 2010 Massachusetts Avenue NW, Washington, DC 20036, USA
[2]Publications Department, The Optical Society, 2010 Massachusetts Avenue NW, Washington, DC 20036, USA
[3]Currently with the Department of Electronic Journals, The Optical Society, 2010 Massachusetts Avenue NW, Washington, DC 20036, USA
**opex@osa.org*

Abstract: Updated 14 June 2017. Explicit and detailed rules are given for preparing a manuscript for OSA express journals. After a general introduction and a summary of the basic requirements, specific guidelines are given for all major manuscript elements (such as abstract, headings, figures, tables, and references) to achieve optimal typographic quality. The use of complete and properly formatted references is particularly important. Adherence to these guidelines will significantly expedite the production of your paper.

OCIS codes: (000.0000) General; (000.2700) General science.

References and links (see Section 4)

1. P. J. Harshman, T. K. Gustafson, and P. Kelley, "Title of paper," J. Chem. Phys. **3**, (to be published).
2. K. Gallo and G. Assanto, "All-optical diode based on second-harmonic generation in an asymmetric waveguide," J. Opt. Soc. Am. B **16**(2), 267–269 (1999).
3. B. R. Masters, "Three-dimensional microscopic tomographic imagings of the cataract in a human lens in vivo," Opt. Express **3**(9), 332–338 (1998).
4. D. Yelin, D. Oron, S. Thiberge, E. Moses, and Y. Silberberg, "Multiphoton plasmon-resonance microscopy," Opt. Express **11**(12), 1385–1391 (2003).
5. B. N. Behnken, G. Karunasiri, D. R. Chamberlin, P. R Robrish, and J. Faist,"Real-time imaging using a 2.8~THz quantum cascade laser and uncooled infrared microbolometer camera,"' Opt. Lett. **33**(5), 440–442 (2008).

1. Introduction

Adherence to the specifications listed in this style guide is essential for efficient review and publication of submissions.

OSA accepts Word and LaTeX submissions. OSA will not publish the same Word file that authors submit for their final revisions, so it is imperative that authors carefully check the final version of their paper before paying the publication fee. OSA uses a Word plug-in to normalize, format, tag, update citations, and parse the file into full-text XML.

Except for numbering and titling of sections, which may not be desirable for short articles, the express journal style and layout rules have been followed in this guide. There is a checklist available in Section 8 that summarizes the style specifications.

2. Page layout and length

Paper size should be U.S. Letter, 21.505 cm x 27.83 cm (8.5 in. x 11 in.). The printing area should be set to 13.28 cm x 21.54 cm (5.25 in. x 8.5 in.); margins should be set for a 3.3-cm (1.3 in.) top and bottom and 4.11-cm (1.625 in.) left and right.

To maintain a rapid publication cycle, the recommended page length for an express journal article is 6 pages. Higher publication fees apply to articles 7–15 pages in length. There is an additional per-page fee for manuscripts longer than 15 pages.

3. Typographical style

The title, author listing and all headers should be in Arial font. The rest of the text and body of the article should be Times New Roman. Please see the checklist in Section 8 that summarizes all of the style specifications.

3.1 Title

Left align the title. The title should be in 16-pt. bold Arial font. Kerning should be set to 16-pt. and spacing expanded by 0.5 in. Use initial cap for first word in title or for proper nouns. Use lowercase following colon. Title should not begin with an article or contain the words "first," "new" or "novel."

3.2 Author names

Left align author names in 12-pt. bold Arial font using small caps. Each express journal has its own color for the author names. Author names should appear as used for conventional publication, with first and middle names or initials followed by surname. Every effort should be made to keep author names consistent from one paper to the next as they appear within OSA publications.

3.3 Author affiliations

All authors and affiliations should be styled in 9-pt. italic Times New Roman font. If all authors share one affiliation, superscript numbers are not needed. The corresponding author will have an asterisk correlating to an email address. All authors must be grouped together using superscripts to callout each affiliation. Hard returns (Enter key) must be used to separate each individual affiliation. Abbreviations should not be used. Please include the country at the end of the affiliation.

AUTHOR ONE[1] AND AUTHOR TWO[2,*]

[1]Peer Review, Publications Department, Optical Society of America, Washington, DC 20036, USA
[2]Publications Department, Optical Society of America, Washington, DC 20036, USA
**opex@osa.org*

Option 1 for affiliation line with two email addresses (only one for the corresponding author):

AUTHOR ONE[1,3] AND AUTHOR TWO[2,*]

[1]Peer Review, Publications Department, Optical Society of America, Washington, DC 20036, USA
[2]Publications Department, Optical Society of America, Washington, DC 20036, USA
[3]xyz@osa.org
**opex@osa.org*

Option 2 for affiliation line with two email addresses (no asterisk used to denote corresponding authorship, implying that the two email addresses share corresponding authorship equally):

AUTHOR ONE[1,3] AND AUTHOR TWO[2,4]

[1]Peer Review, Publications Department, Optical Society of America, Washington, DC 20036, USA
[2]Publications Department, Optical Society of America, Washington, DC 20036, USA
[3]xyz@osa.org
[4]opex@osa.org

3.4 Abstract

Begin the section with the word "**Abstract**:" in bold print followed by a colon. Font size should be 10-pt. and alignment double (left and right) justified.

The abstract should be limited to approximately 100 words. It should be an explicit summary of the paper that states the problem, the methods used, and the major results and conclusions. It also should contain the relevant key words that would allow it to be found in a cursory computerized search. If the work of another author is cited in the abstract, that citation should be written out without a number, (e.g., journal, volume, first page, and year in square brackets [Opt. Express **22**, 1234 (2014)]), and a separate citation should be included in the body of the text. The first reference cited in the main text must be [1]. Do not include numbers, bullets, or lists inside the abstract.

3.5 Copyright

The line immediately following the abstract should be in 8-pt. type.

Please be sure to update this line with the appropriate publication year if needed. Insert a 4-pt. space above and below the copyright line.

3.6 OCIS subject classification

Optics Classification and Indexing Scheme (OCIS) subject classifications should be included at the end of the abstract. OCIS codes should be provided to help with indexing. List the OCIS code in parenthesis, followed by the term spelled out; separate OCIS terms with semicolons. Each paper must contain two to six OCIS codes. Use 8-pt. type for this line. Please avoid using OCIS codes (000.0000) General or (000.2700) General science, and instead customize these codes to best represent the topics of your manuscript.

OCIS codes can be selected during upload. Follow the link for a complete listing.

OCIS codes: (260.1440) Birefringence; (050.1950) Diffraction gratings.

3.7 Main text

The first line of the first paragraph of a section or subsection should start flush left. The first line of subsequent paragraphs within the section or subsection should be indented 0.62 cm (0.2 in.). All main text should be alignment double (left and right) justified.

Section headings may be numbered consecutively and consistently throughout the paper in Arabic numbers and typed in bold. Use an initial capital letter followed by lowercase, except for proper names, abbreviations, etc. Always start headings flush left. Do not include references to the literature, illustrations, or tables in headings. Insert a 6-pt. space above and below each section heading as shown in this paper.

Subsection headings may be numbered consecutively in Arabic numbers to the right of the decimal point, with the section number to the left of the decimal point as shown in this paper. Subsection headings should be in italics, with an initial capital letter followed by lowercase, except for proper names, abbreviations, etc. Start subsection headings flush left. Do not include references to the literature, illustrations, or tables in headings. Create a 6-pt. space above and below each subsection heading as shown in this paper.

Numbering of section headings and subsection headings is optional but must be used consistently throughout papers in which it is applied.

3.8 Equations

The express journals do not accept equations built using the Word 2007 or 2010 Equation Builder. All display equations should be created in MathType (Microsoft Equation Editor 3.0 users are encouraged to use MathType now that Microsoft no longer supports the Equation Editor). Inline equations can be created with these tools or by using keyboard and Unicode characters where needed for the best quality line spacing. We strongly encourage authors to use MathType 6.9. Note that LaTeX users can type LaTeX code directly into MathType for rendering in Word.

Equations should be centered, unless they are so long that less than 1 cm will be left between the end of the equation and the equation number, in which case they may run on to the next line. Equations should have a 6-pt. space above and below the text. Equation numbers should appear at the right-hand margin, in parenthesis. For long equations, the equation number may appear on the next line. For very long equations, the right side of the equation should be broken into approximately equal parts and aligned to the right of the equal sign. The equation number should appear only at the right hand margin of the last line of the equation:

$$\frac{-b \pm \sqrt{b^2 - 4ac}}{2a}. \tag{1}$$

All equations should be numbered in the order in which they appear and should be referenced from within the main text as Eq. (1).

In-line math of simple fractions should use parentheses when necessary to avoid ambiguity; for example, to distinguish between 1/(n – 1) and 1/n – 1. Exceptions to this are the proper fractions such as ½, which are better

left in this form. Summations and integrals that appear within text such as $\frac{1}{2}\sum_{n=1}^{n=\infty}\left(n^2-2n\right)^{1}$ should have limits placed to the right of the symbol to reduce white space. Use MathType or Unicode character sets for in-text and display notation wherever possible.

4. References and links

References should appear at the top of the article, below the abstract, in the order in which they are referenced in the body of the paper (see below). The font should be 8-pt. aligned left. Lines should be single-spaced. The words "**References and links**" should head the section (no number) in bold print followed by one blank line, directly above the first reference. Insert a 6-pt. space above the "**References and links**" line. All references should be indented 0.5 cm (0.2 in), with succeeding lines indented sufficiently to preserve alignment. The references section should be delimited by horizontal rules above and below the section, separated by at least 6-pts. of white space from the text.

OSA express journals use numerical notation in brackets for bibliographic citations. At the point of citation within the main text, designate the reference by typing the number in after the last corresponding word [1]. Reference numbers should precede a comma or period [2]. Two references [3,4], should be included together, separated by a comma, while three or more consecutive references should be indicated by the bounding numbers and an en dash
[1–4].

The express journals follow the following citation style:

Journal paper

For journal articles, authors are listed first, followed by the article's full title in quotes, the journal's title abbreviation, the volume number in bold, the issue number in Roman and parenthesis, inclusive page numbers, and the year in parentheses. Journal titles are required. Do not include DOIs in published journal citations—these will be added post-publication.

1. C. van Trigt, "Visual system-response functions and estimating reflectance," J. Opt. Soc. Am. A **14**(4), 741–755 (1997).
2. S. Yerolatsitis, I. Gris-Sánches, and T. A. Birks, "Adiabatically-tapered fiber mode multiplexers," Opt. Express **22**(1), 608–617 (2014).

Journal paper identified by paper number

Do not provide the number of pages; the paper number is sufficient.

3. L. Rippe, B. Julsgaard, A. Walther, Y. Ying, and S. Kröll, "Experimental quantum-state tomography of a solid-state qubit," Phys. Rev. A **77**, 022307 (2008).

Book

For citation of a book as a whole or book chapter, authors or editors are listed first, followed by title in italics, and publisher and year in parenthesis. Chapter number may be added if applicable.

4. T. Masters, *Practical Neural Network Recipes in C++* (Academic, 1993).
5. F. Ladouceur and J. D. Love, *Silica-Based Buried Channel Waveguides and Devices* (Chapman & Hall, 1995), Chap. 8.

Article in a book

For monographs in books, authors are listed first, followed by article's full title in quotes, the word "in," followed by the book title in italics, the editors of the book, and the publisher and publication year in parenthesis.

6. D. F. Edwards, "Silicon (Si)," in *Handbook of Optical Constants of Solids*, E. D. Palik, ed. (Academic, 1985).

Paper in published conference proceedings

7. R. E. Kalman, "Algebraic aspects of the generalized inverse of a rectangular matrix," in *Proceedings of Advanced Seminar on Generalized Inverse and Applications*, M. Z. Nashed, ed. (Academic, 1976), pp. 111–124.

Paper published in OSA conference proceedings

8. R. Craig and B. Gignac, "High-power 980-nm pump lasers," in *Optical Fiber Communication Conference*, Vol. 2 of 1996 OSA Technical Digest Series (Optical Society of America, 1996), paper ThG1.

Paper in unpublished conference proceedings

9. D. Steup and J. Weinzierl, "Resonant THz-meshes," presented at the Fourth International Workshop on THz Electronics, Erlangen-Tennenlohe, Germany, 5–6 Sept. 1996.

SPIE proceedings

For later SPIE proceedings with a paper number, cite just the paper number and not any page information.

10. S. K. Griebel, M. Richardson, K. E. Devenport, and H. S. Hinton, "Experimental performance of an ATM-based buffered hyperplane CMOS-SEED smart pixel array," Proc. SPIE **3005**, 254–256 (1997).
11. S. Gu, F. Shao, G. Jiang, F. Li, and M. Yu, "An objective visibility threshold measurement method for asymmetric stereoscopic images," Proc. SPIE **8205**, 820505 (2011).

IEEE proceedings

12. T. Darrel and K. Wohn, “Pyramid based depth from focus,” in *Proceedings of IEEE Conference on Computer Vision and Pattern Recognition* (IEEE, 1988), pp. 504–509.

Paper accepted for publication

13. D. Piao, “Cancelation of coherent artifacts in optical coherence tomography imaging,” Appl. Opt. (to be published).
14. D. W. Diehl and T. D. Visser, “Phase singularities of the longitudinal field components in the focal region of a high-aperture optical system,” J. Opt. Soc. Am. A, doc. ID 56789 (posted 11 November 2005, in press).

Manuscript in preparation

15. J. Q. Smith, Laboratory for Laser Energetics, University of Rochester, 250 East River Road, Rochester, N.Y. 14623, and K. Marshall are preparing a manuscript to be called “Optical effects in liquid crystals.”

Personal communication

16. T. Miller, Publications Department, Optical Society of America, 2010 Massachusetts Avenue, NW, Washington, DC 20036 (personal communication, 2010).

Electronic citations

Internet links should list the author, title (or substitute file name, if needed), and the full URL. Include the date of access, if relevant.

17. Extreme Networks white paper, “Virtual metropolitan area networks,” (Extreme Networks, 2001), http://www.extremenetworks.com/technology/whitepapers/vMAN.asp.
18. A. G. Ramm, “Invisible obstacles,” http://www.arxiv.org/abs/math-ph/0608034.

5. Figures, supplementary materials, and tables

5.1 Figures

Figures should be included directly in the document. All photographs must be in digital form and placed appropriately in the electronic document. All illustrations must be numbered consecutively (i.e., not by section) with Arabic numbers. The size of a figure should be commensurate with the amount and value of the information conveyed by the figure.

Authors must use one image file per figure. Figures must be inserted as objects that are fixed and move with the text, not as floating objects. Figures should never be placed in a table environment, embedded inside the text, or included within a list. All the figures should be centered. No part of a figure should go beyond the typing area. Place figures as closely as possible to where they are mentioned in the text. Figures should be numbered consecutively in the order of appearance and citation in the text. Be sure to cite every figure.

All figure captions should be centered beneath the figure. Longer figure captions should be centered beneath the figure and alignment double (left and right) justified, but are not to exceed the left and right edge of the figure by more than 0.5 in. The abbreviation “Fig.” for figure should appear first followed by the figure number and a period. Captions should be in 8- pt. font. At least one line of space should be left before the figure and after the caption.

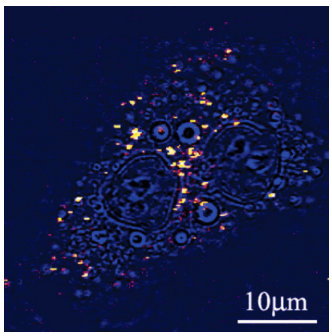

Fig. 1. Sample caption (Ref. [4], Fig. 2).

5.2 Supplementary materials in OSA express journals

Most OSA journals allow authors to include supplementary materials as integral parts of a manuscript. Such materials are subject to the same editorial standards and peer review procedures along with the rest of the paper and should be uploaded and described using OSA’s Prism manuscript system.

Authors can submit appropriate visualizations or small data files (see details below) for OSA to host. Large datasets and code or simulation files can be included but must be placed in an appropriate archival repository and cited as described here.

Table 1. Supplementary Materials Supported in OSA Journals[a]

Visualization	2D image, 3D image, video
Data File	Small data file such as data underlying a plot in a figure
Dataset	Dataset stored in an appropriate external repository
Code	Code or simulation files stored in an appropriate external repository

[a]*Optica* allows authors to include a supplemental document that can contain additional text, equations, citations, etc. (see Supplementary Materials in *Optica* for details). For all other OSA journals, supplemental text must be included as appendices within the primary manuscript.

Video visualizations are the most commonly submitted type of supplementary materials for the express journals. They typically illustrate a synopsis of research results. They are integral and as such should be included only when they convey essential information beyond what can be presented within the article's PDF representation. Video visualizations should be uploaded upon submission and peer-reviewed along with the manuscript. Video files must use open compression standards for display on broadly available applications such as VLC or Windows Media Player. MOV, AVI, MPG, and MP4 video containers are accepted. The following video guidelines will help with the submission process:

1. 15 MB is the recommended maximum video file size.
2. 720 x 480 pixels (width by height) is the recommended screen size.
3. If appropriate, insert a representative frame from the video in the manuscript as a figure.
4. Minimize file size by using an acceptable codec such as x264 or XviD. HandBrake is an open source tool for converting video to common codecs.
5. Videos must be playable on all platforms using VLC.
6. Animations must be formatted into a standard video container.

Visualizations must be associated with a figure, table, or equation OR be referenced in the results section of the manuscript. Use the label "Visualization" and the item number to identify the visualization.

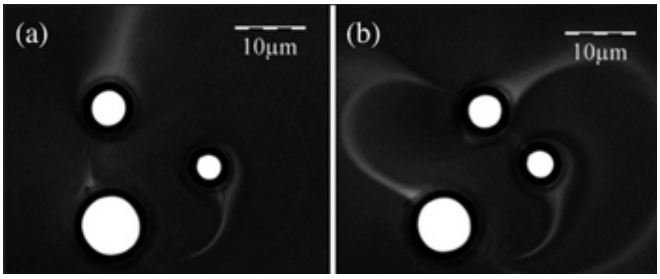

Fig. 5. Three traps create three rings of magnetic nanoparticles. The rings interact with one another (see Visualization 3). [From Masajada *et al.*, Opt. Lett. **38**, 3910 (2013)].

Please refer to the Author Guidelines for Supplementary Materials for more detailed instructions and other acceptable supplementary material types.

5.3 Tables

Tables should be centered and numbered consecutively. Authors must use Word's Table editor to insert tables. Authors must not import tables from Excel. All content for each table should be in a single Word table (do not split content for a single table across multiple Word tables). Tables should use horizontal lines to delimit the top and bottom of the table and column headings. Detailed explanations or table footnotes should be typed directly beneath the table, but not in a table cell. Table footnote labels should be alphabetical; numbers or special characters are not permitted. Position tables as closely as possible to where they are mentioned in the main text.

Table 2. Optical Constants of Thin Films of Materials[a]

	83.4 nm		121.6 nm	
Material	n	K	n	k
Ir	1.182	0.865	1.450	1.040
MgF2	1.584	0.487	1.682	0.0627
Al	0.09874	0.1915	0.0424	1.137
Mo	0.98	1.08	0.78	1.03
C	1.16	1.29	1.85	1.10

[a]From Appl. Opt. **40**, 1128 (2001).

6. Article thumbnail upload

Authors have the option to upload a thumbnail image that will appear next to the published article on the Issue in Progress, Current Issue, and Abstract pages. Please note that if authors do not choose a file, OSA Production Staff will choose an image from the submission. For precise representation of an article, we recommend that authors choose and upload the thumbnail image.

Authors must submit a .JPG file. The image will be resized automatically to 100 x 100 pixels. For best results, authors should upload an image this size or an image with square dimensions.

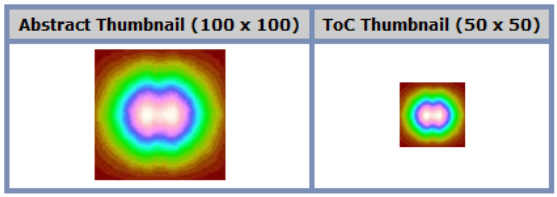

Fig. 3. Preview of thumbnail image display on the author submission page.

7. Funding, acknowledgments, and disclosures

7.1 Funding

Funding information should be listed in a separate block preceding any acknowledgments. The section title should read "**Funding**" in 10-pt. bold Arial font. The section title should not follow the numbering scheme of the body of the paper. List just the funding agencies and any associated grants or project numbers, as shown in the example below:

National Science Foundation (NSF) (1253236, 0868895, 1222301); Program 973 (2014AA014402); Natural National Science Foundation of China (NSFC) (123456).

OSA participates in Crossref's Funding Data, a service that provides a standard way to report funding sources for published scholarly research. To ensure consistency, please enter any funding agencies and contract numbers from the Funding section in Prism during submission. Update any changes to your funding information in Prism during any revision stages.

7.2 Acknowledgments

Acknowledgments should be included at the end of the document. The section title should read "**Acknowledgments**" in 10-pt. bold Arial font. The section title should not follow the numbering scheme of the body of the paper. Please do not include any funding sources in the Acknowledgment section.

7.3 Disclosures

For *Biomedical Optics Express* submissions only, disclosures should be listed in a separate section at the end of the manuscript. The section title should read "**Disclosures**" in 10-pt. bold Arial font. The section title should not follow the numbering scheme of the body of the paper. List the Disclosures codes identified on OSA's Conflict of Interest policy page, as shown in the examples below:

ABC: 123 Corporation (I,E,P), DEF: 456 Corporation (R,S). GHI: 789 Corporation (C).

If there are no disclosures, then list "The authors declare that there are no conflicts of interest related to this article."

8. Summary

Conforming to the specifications listed above is of critical importance to the speedy publication of a manuscript. Authors should use the following style guide checklist before submitting an article.

Table 3. Style Guide Checklist

Standard Page Text Area: 5.25 x 8.5 in.; Margins: 1.3 in. top and bottom, 1.625 in. left and right				
Type of Text	**Font**	**Font Size (Points)**	**Alignment**	**Notes**
Title	Arial	16	Left	**Bold** Spacing expanded by 0.5 pts. Kerning 16 pts
Author Name	Arial	12	Left	**Bold** Use SMALL CAPS Use journal color
Affiliation & Email	Times New Roman	9	Left	*Italic*
Abstract	Times New Roman	10	Justified	Bold "**Abstract:**" header
Copyright	Times New Roman	8	Left	
OCIS Codes	Times New Roman	8	Left	Bold "**OCIS codes:**" header
Main Text First paragraph Subsequent paragraphs	Times New Roman	10	Justified	The first paragraph of a section or subsection is not indented. The first line of subsequent paragraphs is indented 0.2 in.
Section & Subsection Headings	Arial	10	Left	Insert 6-pt. space above and below each heading. Section headers: **Bold** Subsection headers: *Italic*
Equations		10	Center	Eq. Number: right tab to end of last line of Eq., in parentheses.
References and links	Times New Roman	8	Left	Bold "References and links". Delimit with horizontal rules.
Funding	Times New Roman		Justified	Bold "**Funding**" section header
Acknowledgments	Times New Roman	10	Justified	Bold "**Acknowledgments**" section header
Disclosures	Times New Roman	10	Justified	Bold "**Disclosures**" section header
Figures			Center	
Figure Captions	Times New Roman	8	Justified	Long captions: indent 0.5 in. left/ right.
Tables	Times New Roman	8	Center	**Table 1. Bold table captions**
Table Heads	Times New Roman	8	Center	Long heads follow table margins.

Autorització per a la difusió de treballs acadèmics (TFG, TFM, etc.) a través del dipòsit institucional *UPCommons*

***IDIOMA DEL TFC** ANGLÈS*

1. Difusió pública del treball acadèmic

"Els titulars de la propietat intel·lectual dels treballs acadèmics dirigits o coordinats per professorat de la UPC són els estudiants autors del mateixos que, com a tals, són qui els poden reproduir, distribuir, comunicar públicament, transformar i/o cedir-ne els drets d'explotació a tercers." .... Propietat industrial i intel·lectual dels treballs acadèmics presentats a la UPC (TFG PFM, tesines, tesis doctorals, etc.)" de la web del Servei de Biblioteques: http://publica.upc.edu/copyright/tfg

En/Na DANIEL ESPINAR MARTÍNEZ DNI/Passaport núm. 53833619A, autor/a del treball acadèmic titulat "MORPHOLOGICAL ANALYSIS FOR IMPROVING CLINICAL DIAGNOSIS OF SKIN CANCER"

( ) **AUTORITZO** la comunicació pública de les dades bibliogràfiques i del text complet del treball en xarxa a través del dipòsit institucional *UPCommons* o plataforma que el substitueixi. Aquesta difusió només es portarà a terme sempre i quan el corresponent professor director, coordinador o tutor n'hagi descartat un tractament confidencial.
(Si es marca aquesta opció, és obligatori escollir una llicència Creative Commons -punt 2- i emplenar també, obligatòriament, el punt 3 de l'adreça de correu electrònic personal (que vol dir que l'adreça de correu electrònica es farà pública o no, juntament amb la resta de dades del TFC que si es faran públiques, per si alguna persona vol posar-se en contacte amb ell).

(X) **NO AUTORITZO** la comunicació pública del text complet del treball, motiu pel qual el Servei de Biblioteques, Publicacions i Arxius de la UPC només difondrà a UPCommons les corresponents dades bibliogràfiques. Aquesta difusió només es portarà a terme sempre i quan el corresponent professor director, coordinador o tutor n'hagi descartat un tractament confidencial.
(Si es marca aquesta opció, el punt 2 s'ha de deixar en blanc, però sí ha d'omplir obligatòriament el punt 3 de l'adreça de correu electrònic personal, pel mateix motiu que en l'apartat anterior)

Si és confidencial, cal aportar la clàusula de confidencialitat.

2.Atorgament d'una llicència Creative Commons *[ompliu aquest apartat només si heu autoritzat la difusió del text complet del treball en xarxa]*

El sotasignat autoritza la difusió del treball acadèmic:

( ) mitjançant la llicència CC **"Reconeixement-NoComercial-SenseObraDerivada"** (by-nc-nd)
[permet reproduir, distribuir, comunicar públicament però no fer obres derivades (traduccions, etc.), sempre i quan s'esmenti l'autoria i no es facin usos comercials]
( ) mitjançant la llicència CC **"Reconeixement-NoComercial-CompartirIgual"** (by-nc-sa)
[permet reproduir, distribuir, comunicar públicament i fer obres derivades (traduccions, etc.), sempre i quan s'esmenti l'autoria i no es facin usos comercials]
( ) **sense aplicació de cap llicència CC**
[les condicions d'ús del treball dipositat són únicament les permeses per la Llei de propietat intel·lectual (BOE núm. 97, de 22/4/1996)]

3. Difusió pública d'una adreça de correu electrònic

El sotasignant autoritza la difusió del registre bibliogràfic del seu treball:

( ) **amb l'adreça de correu electrònic**
[s'ofereix una adreça de contacte que permeti la futura comunicació entre l'autor i els investigadors, empresaris o altres possibles usuaris interessats en la seva obra]

( ) **sense cap adreça de correu electrònic** *[no s'ofereix cap adreça de contacte]*

En cap cas aquesta autorització implica una cessió en exclusiva dels drets d'explotació de l'autor/a sobre l'obra ni impedeix l'explotació normal de l'obra a través de les formes habituals.
La durada de l'autorització serà indefinida, excepte revocació expressa per part dels titulars dels drets i/o incompliment de qualsevol de les parts de les obligacions contingudes a la mateixa
L'autor/a declara que és el legítim propietari dels drets d'autor de l'obra que s'autoritza. Si el document inclou obres de les quals no n'és el propietari dels drets d'explotació (fotografies, dibuixos, textos, etc.), l'autor/a declara que ha obtingut el permís sense restricció del titular corresponent per atorgar la present autorització.

Terrassa, 7 de Juny de 2018

Signatura de l'autor/a:

En compliment del que estableixen la *Llei orgànica 15/1999, de 13 de desembre sobre protecció de dades de caràcter personal* i el *Reial Decret que aprova el Reglament de desenvolupament de la Llei Orgànica de Protecció de dades de caràcter personal*, us informem que les vostres dades personals recollides per mitjà d'aquesta autorització seran tractades i quedaran incorporades als fitxers de la Universitat Politècnica de Catalunya (UPC) per dur a terme una gestió correcta de la prestació de serveis bibliotecaris. Tanmateix, us informem que podeu exercir els drets d'accés, rectificació, cancel·lació i oposició davant del Servei de Biblioteques, Publicacions i Arxius, amb domicili a: Campus Nord UPC, edifici TG. C/Jordi Girona, 31. 08034 Barcelona, a l'adreça de correu electrònic: info.biblioteques@upc.edu.

Així mateix, consentiu de manera expressa que les vostres dades siguin cedides als estaments oficials públics oportuns i necessaris, i amb la finalitat de garantir la correcta prestació dels serveis autoritzats. Aquest consentiment podrà ser revocat en qualsevol moment.

Declaración de confidencialidad de los Trabajos académicos (TFG, TFM, etc.)

Declaración de confidencialidad

Don/doña MERITXELL VILASECA, como profesor/a responsable de la dirección, coordinación y/o tutoría del Trabajo académico depositado por el estudiante DANIEL ESPINAR MARTÍNEZ titulado "MORPHOLOGICAL ANALYSIS FOR IMPROVING CLINICAL DIAGNOSIS OF SKIN CANCER" declaro que:

(X) El trabajo académico **es confidencial** (según las condiciones detalladas a continuación)
( ) El trabajo académico **no es confidencial**

Período y motivos de la confidencialidad

[Cumplimentar este apartado sólo si ha declarado que el trabajo es confidencial]

El abajo firmante declara que el trabajo académico ha de ser confidencial por el período de tiempo que a continuación se indica:

(X) **Hasta la fecha** 15 de JUNIO de 2022
( ) La duración de la confidencialidad **es indefinida**

El abajo firmante declara que los motivos de esta confidencialidad son:

( ) Se quiere evaluar la posibilidad de proteger el trabajo
( ) Un tercero manifiesta interés en comercializar el trabajo
( ) Forma parte de un trabajo de investigación con una empresa que está sujeta a confidencialidad
(X) Otros: Publicación en una revista de investigación.

Difusión pública del trabajo confidencial

[Cumplimentar este apartado sólo si ha declarado que el trabajo es confidencial]

El abajo firmante autoriza la difusión del trabajo confidencial al depósito institucional en *UPCommons* o plataforma que lo substituya bajo estas condiciones:
( ) Difusión del **texto completo del trabajo** a partir de la fecha de embargo indicada en el apartado anterior (siempre y cuando el autor del trabajo autorice esa difusión)
( ) Difusión única de los **datos bibliográficos** del trabajo (sin el texto completo)
(X) La confidencialidad del trabajo no permite **ninguna difusión** del mismo

> En el caso de que la confidencialidad del trabajo no permita ninguna difusión del mismo, el Servicio de Bibliotecas, Publicaciones y Archivos de la UPC, acogiéndose al artículo 37.1 de la Ley de Propiedad Intelectual, depositará en cerrado el proyecto en *UPCommons* (sin ningún acceso público al texto ni correspondientes datos bibliográficos), garantizando así su confidencialidad, preservación y conservación.

Terrassa, 7 de Junio de 2018

Firma del profesor director, coordinador y/o tutor:

En cumplimiento de lo establecido en la *Ley Orgánica 15/1999, de 13 de diciembre sobre protección de datos de carácter persona*l y *el Real Decreto que aprueba el Reglamento de desarrollo de la Ley Orgánica de Protección de datos de carácter personal*, le informamos de que sus datos personales recogidos por medio de esta autorización serán tratados y quedarán incorporados a los ficheros de la Universidad Politécnica de Cataluña (UPC) para llevar a cabo una gestión correcta de la prestación de servicios bibliotecarios. Sin embargo, le informamos que puede ejercer los derechos de acceso, rectificación, cancelación y oposición ante el Servicio de Bibliotecas, Publicaciones y Archivos, con domicilio en: Campus Nord UPC, edificio TG. C / Jordi Girona, 31. 08034 Barcelona, en la dirección de correo electrónico:info.biblioteques@upc.edu.

Asimismo, acepta de manera expresa que sus datos sean cedidos a los estamentos oficiales públicos oportunos y necesarios, y con el fin de garantizar la correcta prestación de los servicios autorizados. Este consentimiento podrá ser revocado en cualquier momento.